Fractionated Crystallization of Dispersed PA6 Phase of PP/PP-*g*-MAH/PA6 Blends

Dean Shi,[1,2,*] Jinghua Yin,[1] Zhuo Ke,[1] Ying Gao,[1] R. KY Li[3]

[1]*State Key Laboratory of Polymer Physics and Chemistry, Changchun Institute of Applied Chemistry, Chinese Academy of Sciences, Changchun 130022, People's Republic of China*
[2]*Faculty of Chemistry and Material Science, Hubei University, Wuhan, 430062, People's Republic of China*
[3]*Department of Physics and Material Science, City University of Hong Kong, Tat Chee Avenue, Kowloon, Hong Kong, People's Republic of China*

Received 23 December 2002; accepted 27 August 2003

ABSTRACT: Fractionated crystallization behavior of dispersed PA6 phase in PP/PA6 blends compatibilized with PP-*g*-MAH was investigated by scanning electron microscopy (SEM), differential scanning calorimeter (DSC), polarized light microscopy (PLM), and wide-angle X-ray diffraction (WAXD) in this work. The lack of usual active heterogeneities in the dispersed droplet was the key factor for the fractionated crystallization of PA6. The crystals formed with less efficient nuclei might contain more defects in the crystal structures than those crystallized with the usual active nuclei. The lower the crystallization temperature, the lesser the perfection of the crystals and the lower crystallinity would be. The fractionated crystallization of PP droplets encapsulated by PA6 domains was also observed. The effect of existing PP-*g*-MAH-*g*-PA6 copolymer located at the interface on the fractionated crystallization could not be detected in this work. © 2004 Wiley Periodicals, Inc. J Appl Polym Sci 91: 3742–3755, 2004

INTRODUCTION

Since the fractionated crystallization of a semicrystalline polymer suspended in an inert liquid was observed,[1] many researchers have paid much attention on investigating this crystallization behavior.[2–19] The nucleation process in crystallizable polymers usually occurs by one or more of the following: homogeneous nucleation, heterogeneous nucleation, or self-nucleation. Generally, semicrystalline polymers in the bulk nucleate on existing heterogeneous (catalyst debris, impurities, and others). However, if the bulk polymer is subdivided into isolated regions (like, for instance, droplets in an immiscible matrix in the case of polymer blends), whose number is significantly greater than usually active heterogeneities at low super cooling, a fractionated crystallization phenomenon may occur.[1,2] When such a dispersion within an amorphous matrix is cooled from the melt, a series of crystallization exotherms can be observed, which have been interpreted as the crystallization of different groups of droplets at specific and independent supercoolings. The droplets containing heterogeneities, which are usually active at low supercoolings in the bulk polymer, will crystallize at a temperature identical to that of the polymer in the bulk. Droplets containing other types of less efficient heterogeneities will nucleate at higher supercooling necessary for those heterogeneities to become active. Finally, those droplets that do not contain any heterogeneity will only nucleate with the most supercooling, because greater supercooling is usually needed to generate homogeneous nuclei.

The fractionated crystallization process will be prevented, if the matrix can nucleate along with the dispersed phase. In that case, the possibility of coincident crystallization depends on the relative crystallization temperatures of the two components.[2,4]

In recent years, the fractionated crystallization behavior of polyamide 6 in polypropylene/polyamide 6 (PP/PA6) blending system has been widely studied by several research groups.[7,9,11,13] Jafari et al [9] found, that in the PP/PA6 blends, the crystallinity of both components were not in the same proportion as their weight fractions in a blend. The crystallinity of PP decreased in the presence of PA6, whereas the crystallinity of PA6 increased considerably in the presence of PP. Ikkala et al.[7] studied the fractionated crystallization behavior of PP/PA6 blends by using polypropylene grafted maleic anhydride (PP-*g*-MAH), ethyl-

*Working as a Research Fellow in City University in Hong Kong.

Correspondence to: J. Yin (yinjh@ciac.jl.cn).

Contract grant sponsor: the National Science Foundation of China for the Special Funds for Major State Basic Research Projects; contract grant number: G19990648.

Contract grant sponsor: the Major Program; contract grant number: 50290090.

Contract grant sponsor: the General Program; contract grant number: 59873022.

Contract grant sponsor: the Wuhan Youth Scheme of Science and Technology; contract grant number: 20025001012.

Journal of Applied Polymer Science, Vol. 91, 3742–3755 (2004)

ene butylene acrylate grafted fumaric acid (EBA-*g*-FA), styrene ethylene butylene styrene elastomer grafted maleic anhydride (SEBS-*g*-MAH), and ethylene ethyl acrylate grafted glycidyl methacrylate (EEA-*g*-GMA) as compatibilizers, respectively. They found that the compatibilized blends showed more complex crystallization behavior compared with the corresponding binary blends. In the compatibilized blending system, the dispersed PA6 phase seemed to crystallize coincidentally with PP. The crystallization of PP, in blends compatibilized with PP-*g*-MAH and blends without any compatibilizer, took place at a temperature that was higher than the crystallization temperature of the pure PP. By contrast, in blends compatibilized with EBA-*g*-FA, SEBS-*g*-MAH, and EEA-*g*-GMA, the crystallization of PP took place either at the temperature at which pure PP crystallized or at the temperature range of 76–87°C. Moon et al.[13] studied the effects of the concentration of PP-*g*-MAH on the crystallization behavior of PP/PA6 blends. They found that the crystallization temperature of PA6 dropped down as the concentration of PP-*g*-MAH increased, whereas that of PP stayed at a roughly constant temperature. They also found that with increasing the PP-*g*-MAH content the crystallinity of PA6 decreased, but the melting point of PA6 remained unchanged.

It is well known that the end amino groups of PA6 molecules could react with the anhydride group of the PP-*g*-MAH during the melt processing[20] and form the PP-*g*-MAH-*g*-PA6 copolymer. Moon et al.[13] suggested that the fractionated crystallization behavior was due to the reduction of the dispersed phase's particle size rather than the constraint effect of the PP-*g*-MAH-*g*-PA6 copolymer. They also ascribed the decrease of crystallinity of PA6 in the PP/PA6 blends to the formation of γ-form PA6 crystals. Sánchez et. al.[19] also reported on the γ-form of PA6 crystals in the PA6/ULDPE blends with ULDPE-graft-DEM (diethylmaleate) as a compatibilizer. But Ikkala et al.[7] thought that the fractionated crystallization could not be solely attributed to the size of the dispersed particles. Fractionated crystallization might yield information on the characteristic interfacial energies between polymeric components in the blend.

In this article, the fractionated crystallization behavior of PA6 in PP/PP-*g*-MAH/PA6 blends was studied. Much attention was paid to the effect of different heterogeneous nuclei contents on fractionated crystallization of the PA6 microdomains in the blending system.

TABLE I
Compositions of Samples of PP/PP-*g*-MAH/PA6 Blends before and after Extractions with Formic Acid

Sample Code	PP/PP-*g*-MAH/PA6 (before extraction) wt %	(PP+PP-*g*-MAH)/PA6 (after extraction) wt %
A	40/40/20	80/20
B	0/80/20	80/20
C	0/70/30	78.0/22.0
D	0/60/40	80.4/19.6
E	0/60/40	85.0/15.0
F	0/60/40	88.8/11.2

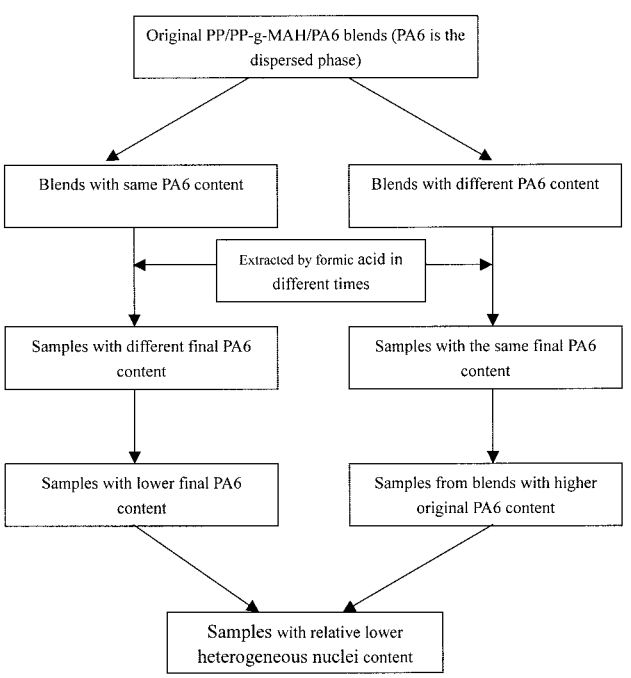

Scheme 1 Preparing procedures of a series of PP/PP-*g*-MAH/PA6 blends with different contents of the PP-*g*-MAH-*g*-PA6 copolymer.

EXPERIMENTAL

Materials

Polyamide 6 (PA6) was supplied by Heilongjiang Nylon Plastic Factory, China. Its relative viscosity was 2.5 (1 g/100 mL formic acid solution 30°C), and $\bar{M}_n = 2.4 \times 10^4$. Isotactic polypropylene was supplied by Beijing Yanshan Petrochemical Co. Ltd, China. Its commercial code is 2401 and MFR is 7.9 g/10 min. Polypropylene grafted with maleic anhydride (PP-*g*-MAH) (CA-100) was supplied by Elf Atochem. The grafting degree of MAH was 1.03% by weight and MFR = 100 g/10 min. Formic acid, acetone, and alcohol were all reagent grades and were used without any further purification.

Preparation of PP/PP-*g*-MAH/PA6 blends

PP/PP-*g*-MAH/PA6 blends were prepared by using an internal mixing chamber (Brabender Plasticorder PLE 330). Before blending, PP, PP-*g*-MAH, and PA6 were dried in a vacuum oven at 70°C for about 24 h. The mixing temperature was 230°C.The rotating rate of rotors was 50 rpm, and the mixing time was 7 min.

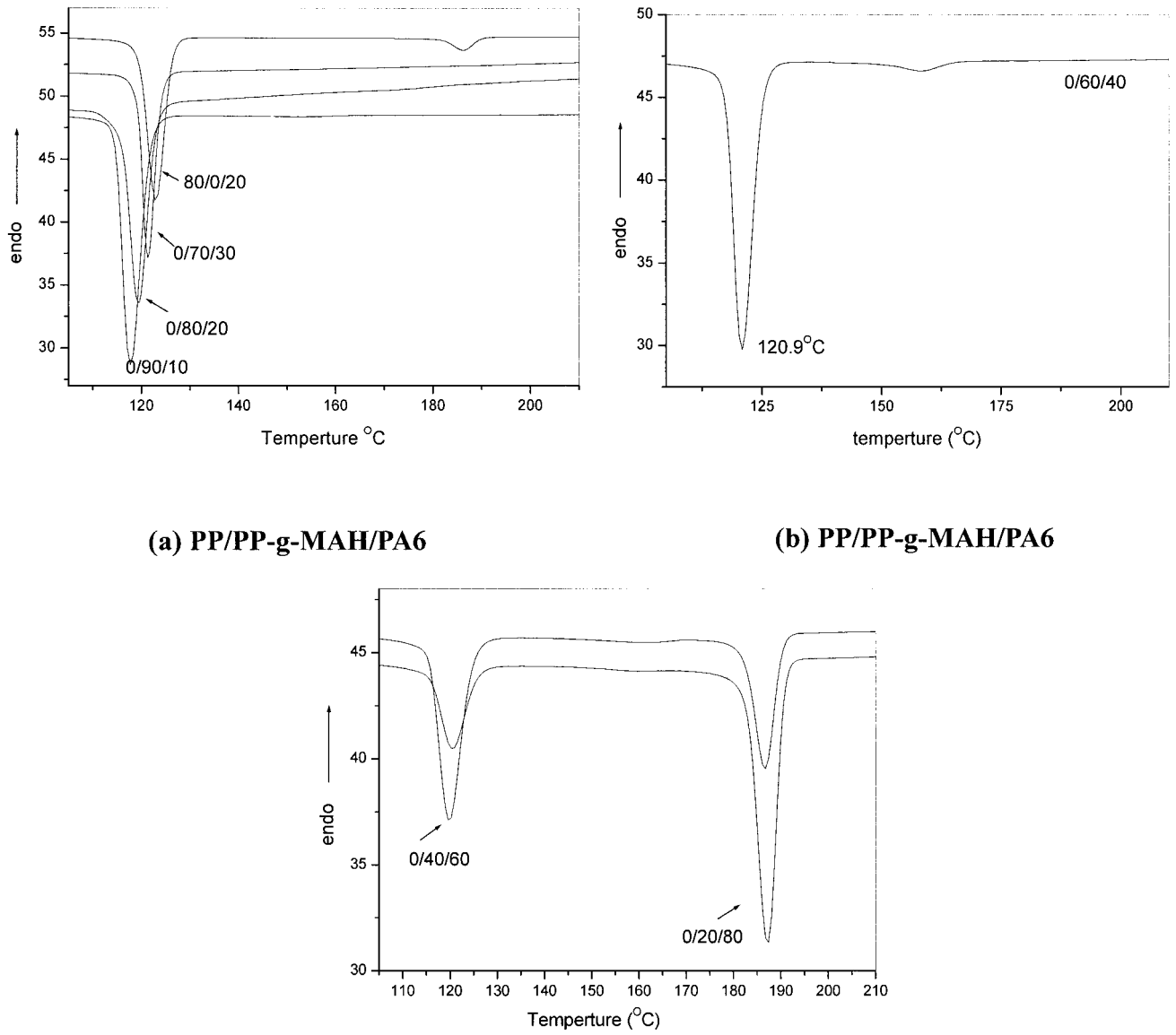

Figure 1 DSC cooling scans (10°C/min) of PP/PP-*g*-MAH/PA6 blends with different compositions (erasing the thermal history by heating to 250°C and holding for 5min and then cooling to room temperature at 10°C/min before testing).

Preparation of blends containing different contents of heterogeneous nuclei

To get blended samples with different amounts of heterogeneous nuclei, boiling formic acid was used to extract the original blends. PA6 could be partially dissolved in this solvent. The total heterogeneous nuclei content would decrease with the dissolation of the PA6 phase during extraction. We could get blend samples with different heterogeneous nuclei content in the following way, shown in Scheme 1. Original blends with compositions of PP/PP-*g*-MAH/PA6 = 0/70/30 and 0/60/40 (all the blends compositions in the latter part of this article will only be listed in the abbreviated form) were extracted by formic acid to samples with the same PA6 content (~20% wt), sample C and D in Table I. We could easily find that the total number of heterogeneous nuclei in sample D was smaller than that in sample C, because more PA6 was removed in sample D The heterogeneous nuclei in samples C and D were all much smaller than that in samples A and B. If sample D was further extracted to samples E and F, which contained even less PA6 component, far fewer heterogeneous nuclei should have remaine. So, the total number of impurities or heterogeneities in the blends decreased in the trend from sample B to sample F (A ~ B > C > D > E > F).

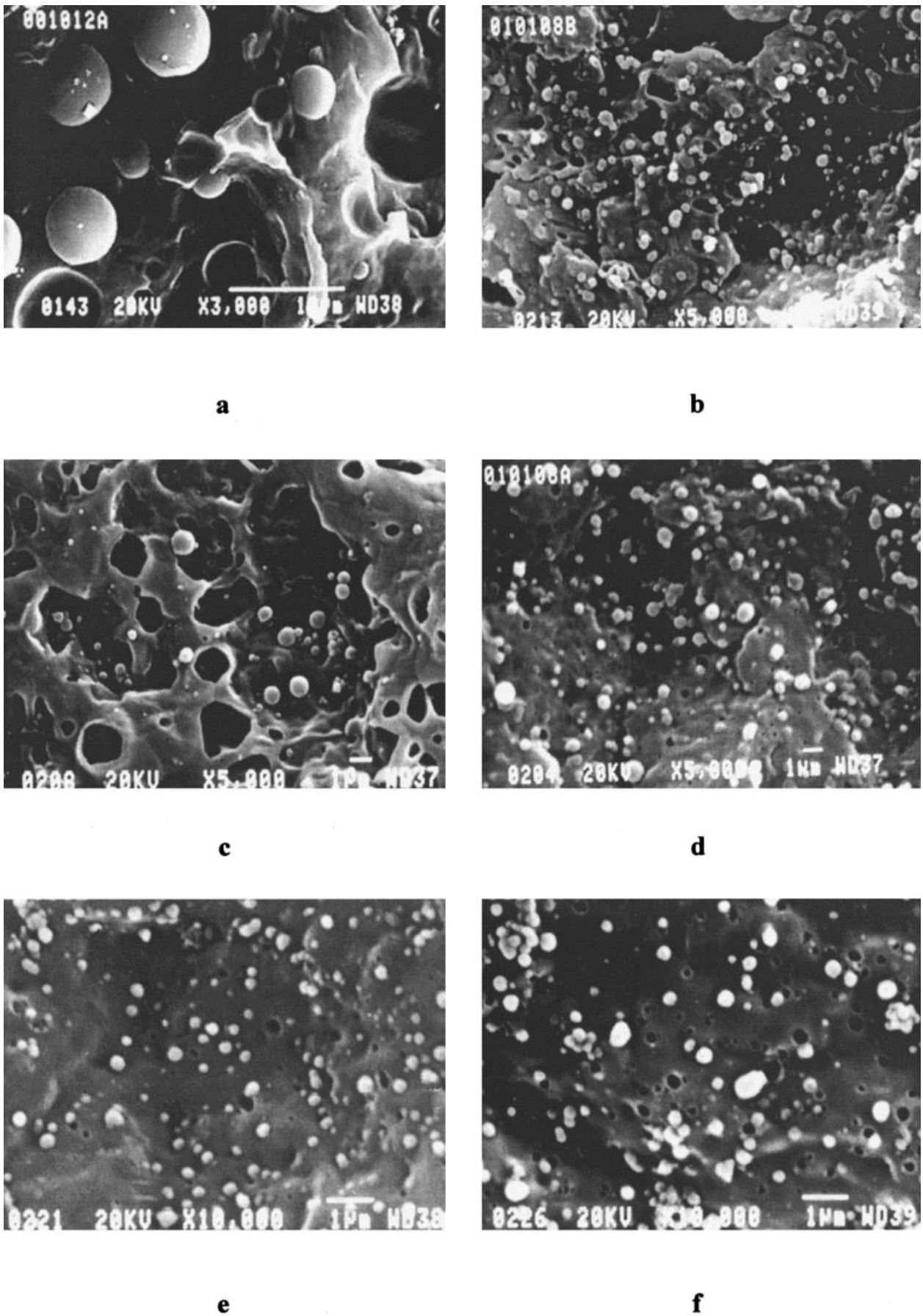

Figure 2 SEM micrographs of PP/PP-*g*-MAH /PA6 blends. (a) 80/0/20; (b) 0/40/60; (c) 0/60/40; (d) 0/70/30; (e) 0/80/20; (f) 0/80/20 (extracted from original sample 0/60/40).

TABLE II
Average Particle Size and Its Distribution of PP/PP-*g*-MAH/PA6 Blends with Different Compositions

Picture code in Figure 3	PP/PP-*g*-MAH/PA6 (wt %)	d_v (μm)	D (dispersity)
a	80/0/20	18.9	1.8
b	0/40/60	—	
c	0/60/40	1.92	1.2
d	0/70/30	0.32	1.05
e	0/80/20	0.2	1.02
f	0/80/20[a]	0.2	1.02

[a] Extracted by formic acid from original composition 0/60/40.

Analysis of the content of PA6 in blending samples

The content of PA6 of blending samples was obtained by determining the content of elemental nitrogen. A Vario EL CHNOS Elemental Analyzer (elementar Analysensysteme GmbH) was used in this work. A sample was digested by using oxidative combustion. The quantitative digestion is based on the principal of explosive combustion in a highly oxygenated helium atmosphere and carried out in a combustion tube filled with CuO of a temperature of 950–1000°C. A thermal conductivity detector (TCD) with a wide dynamic range and improved sensitivity to the carrier gas helium, served as the detector module.

Determination of thermal properties of blending samples

Thermal properties of PP/PP-*g*-MAH/PA6 samples were measured by DSC (Perkin-Elmer DSC-7) under nitrogen atmosphere. Indium was used to calibrate temperature and the heat of fusion. The weight of each sample was about 6–8 mg. The testing temperature range was 0–250°C, and the heating or cooling rates were 10°C/min.

Characterization of crystalline structure of PA6 in PP/PP-*g*-MAH/PA6 blends

Wide-angle X-ray diffraction patterns of the pure PA6 and PA6 in PP/PP-*g*-MAH/PA6 blends were recorded by using a Phillips PW1700 X-ray diffractom-

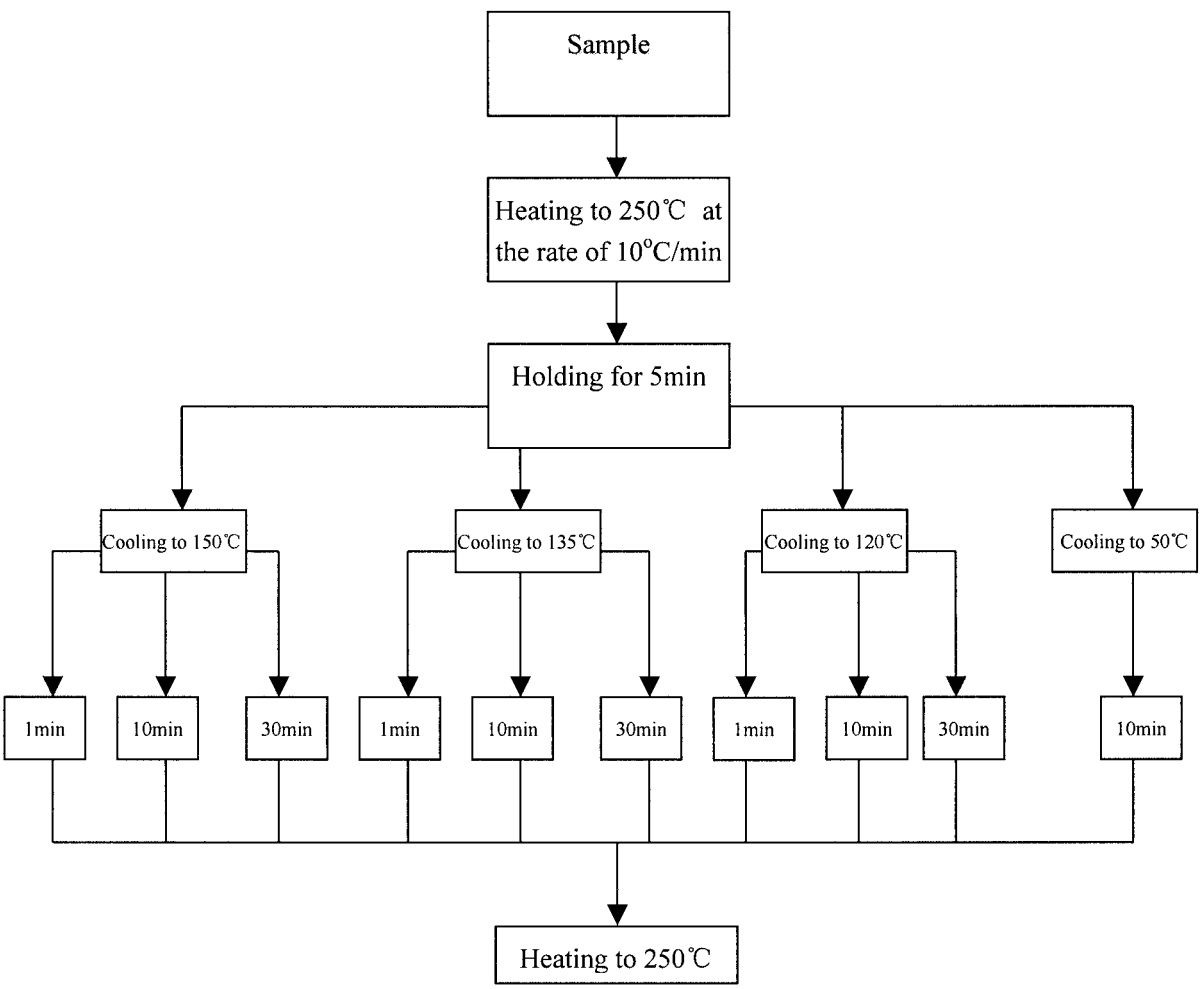

Scheme 2 DSC testing procedures of PP/PP-*g*-MAH/PA6 blends with different compositions.

TABLE III
Melting Enthalpy (ΔH_m) of PP/PP-*g*-MAH/PA6 Blends with Different Compositions Obtained at Different Annealing Temperatures

Sample (original PA6 wt %)	PA6 (wt %) content	ΔH_m (J/g) 50°C	ΔH_m (J/g) annealing at 120°C			ΔH_m (J/g) annealing at 135°C			ΔH_m (J/g) annealing at 150°C		
			1 min	10 min	30 min	1 min	10 min	30 min	1 min	10 min	30 min
B (20)	20.0[a]	68.8	68.2	68	69	19.2	19.8	19.0	7.0	7.2	7.6
C (30)	22.0	62.4	59.0	62	60	15.1	15.4	15.6	6.0	6.6	6.4
D (40)	19.6	55.0	55.0	55	56	11.3	11.0	11.2	5.0	5.1	5.5
E (40)	15.0	55.3	52.0	56	55	7.0	6.8	6.8	2.9	3.0	2.6
F (40)	11.2	51.5	52.5	53	51	6.3	6.0	6.1	2.1	2.4	2.1

[a] Unextracted sample.

eter. Measurement was carried out with Cu target, K_α radiation. The operating voltage was 45 kV, and tube current was 40 mA. Graphite crystal was used as a monochromator. The scanning range was 5–35° with the rate of 0.1°/min. To eliminate the thermal history, all the samples were heated to 250°C and held for 3 min. The test was taken at 180°C to destroy the PP crystals completely.

Observation of morphology of blending samples

A Leica optical microscopy equipped with crossed polarizers and a hot stage was used to observe the morphology of crystallized components in the blended samples at different temperatures. All the samples were preheated to 250°C to eliminate the thermal history. A scanning electron microscope (JEOL JXA-840) was used to examine the size of domains and their size distribution on the fracture surface of the blended samples. The number average and volume average diameters (d_n and d_v) of the particle cross-sectioned surfaces were calculated by measuring and counting at least 100 particles in the micrographs. The dispersity of the particle size (D) was defined as $D = d_v/d_n$. The number and volume average diameters were obtained using the following equations:[21]

$$d_n = \sum n_i d_i / \sum n_i \quad (1)$$

$$d_v = \sum n_i d_i^4 / \sum n_i d_i^3 \quad (2)$$

RESULTS AND DISCUSSION

Fractionated crystallization behavior of PA6 in PP/PP-g-MAH/PA6 blends was observed when PA6 was the dispersed phase. As shown in Figure1(b), the crystallization peak of PA6 in the blend 0/60/40 shifted towards low temperature. With further decrease in the content of PA6 of blends (0/70/30, 0/80/20, and 0/90/10) no independent exothermic peak of PA6 could be found; the crystallization peak of PA6 was combined with the crystallization peak of PP and shifted to a lower temperature. In blends 0/40/60 and 0/20/80, when PA6 became the continuous phase, the usual crystallization peak of PA6 appeared again [Fig. 1(c)]. This phenomenon could be easily explained by the typical fractionated crystallization theory. When the particle size decreased in the compatibilized system, its number would increase, which would result in the total number of disperse particles being greater than that of the usual active nuclei in the system. Only droplets containing the usual active heterogeneities could crystallize at normal bulk crystallization temperature. As this part of the exotherm was too small for DSC to detect, no signals could be found at the normal crystallization temperature position. Most PA6 crystallization should be activated by less active heterogeneous nuclei—crystallized at a lower temperature than normal [Fig. 1(b)] or induced by PP crystallization during the cooling procedure—crystallized coincidentally with PP [Fig. 1(a)]. Here we also no-

TABLE IV
Melting Temperature (T_m) of PP/PP-*g*-MAH/PA6 Blends with Different Compositions Obtained at Different Annealing Temperature

Sample (original PA6 wt %)	PA6 (wt %) content	T_m (°C) heating from 50°C	T_m (°C) annealing at 120°C			T_m (°C) annealing at 150°C		
			1 min	10 min	30 min	1 min	10 min	30 min
B (20)	20.0[a]	219	219	219	219	212	212	212
C (30)	22.0	218	217	217	217	211	211	211
D (40)	19.6	216	213	213	213	210	210	210
E (40)	15.0	214	211	211	211	205	205	205
F (40)	11.2	205	198	198	198	194	194	194

[a] Unextracted sample.

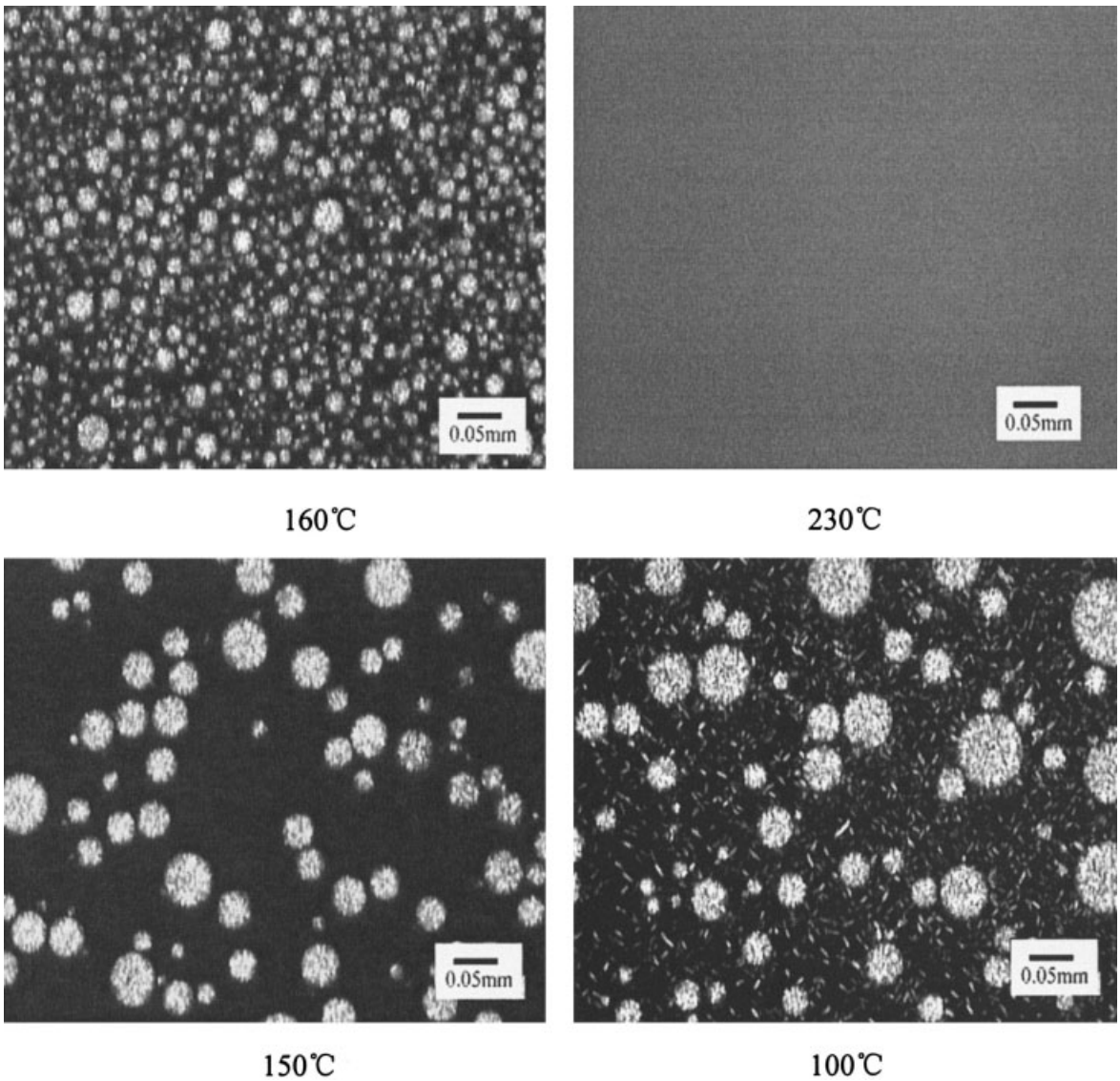

Figure 3 PLM micrographs of PP-*g*-MAH-*g*-PA6/PA6 blends. (a) 80/0/20; (b) 40/40/20; (c) 0/80/20; (d) 0/80/20 (extracted PP/PP-*g*-MAH/PA6 = 0/60/40).

ticed that, even in the 0/70/30 blend, the crystallization peak of PP was somewhat lower than that in the uncompatibilized 80/0/20 blend [see Fig. 1(a)]. A tentative explanation of this phenomenon will be given in the latter part of this article.

SEM micrographs of the PP/PP-*g*-MAH/PA6 blends are shown in Figure 2. The average diameter of the dispersed PA6 particles and the size distribution decreased sharply when PP was replaced by PP-*g*-MAH. As shown in Figure 2(a) and Table 2, the average volume diameter of PA6 particles was 18.9 μm for the 80/0/20 blend, and 0.2 μm for the 0/80/20 blend, respectively. Meanwhile, the dispersity of the size distribution decreased from 1.8 to 1.02, indicating that the size of the PA6 particles was the prerequisite for its fractionated crystallization. But it was also noticed that, in our system, the dispersed droplets size did not change much with the fractionate crystallization. It is well known that the key mechanism of fractionated crystallization was the lack of usual active heterogeneities in the dispersed particles. So, the first thing to do was to determine the difference of crystallization behavior in the blending system with similar dispersed droplet size but a different total number of active heterogeneities.

Crystallization behaviors of Sample B, C, D, E, and F, with different total amounts of heterogeneities, were investigated by using DSC. The experimental procedures are shown in Scheme 2. First, all samples were heated to 250°C and held at this temperature for 5 min, then, samples were cooled to 150, 135, and 120°C, respectively. All samples were annealed at each temperature for 1, 10, and 30 min. Finally, the annealed samples were heated again to 250°C. Melting temperature (T_m) and melting enthalpy (ΔH_m) of PA6 in all annealed samples are given in Table 3 and Table

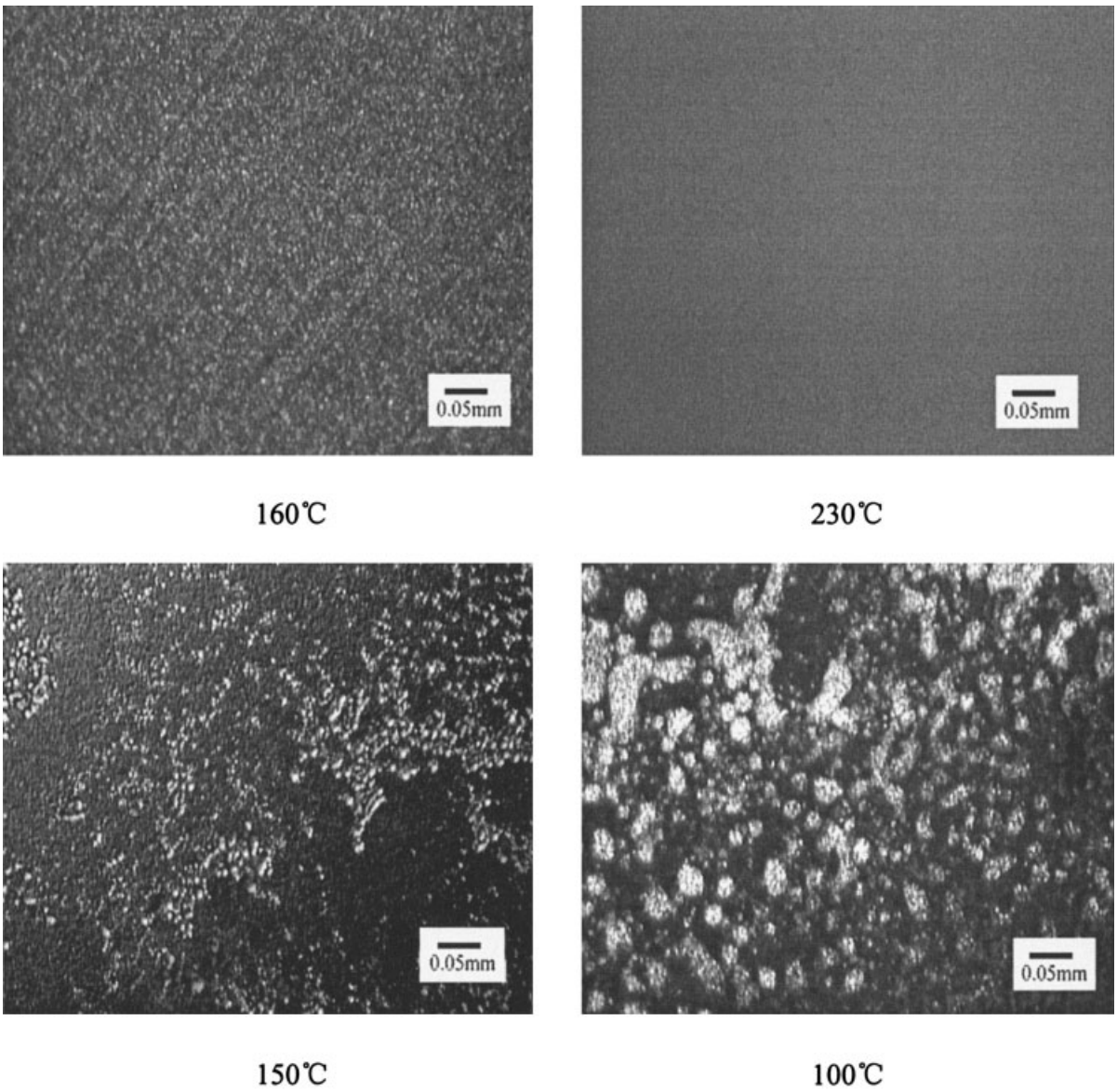

Figure 3 (*Continued from the previous page*)

4. It was found that in all samples some of the dispersed PA6 droplets crystallized at 135 and 150°C. This feature was very similar to that observed in PVDF/PA6 blends by Ikkala et al.[7] For a given sample, the ΔH_m of PA6 particles decreased with increasing annealing temperature. This could be attributed to the particular fractionated crystallization phenomenon. When the number of the usually active nucleating heterogeneities was much smaller than that of the dispersed PA6 droplets, some particles crystallized at a higher supercooling temperature with less active heterogeneities. So, the lower the annealing temperature, the more active nuclei and the higher the total PA6 crystallinity (ΔH_m) would be. At the annealing temperature of 120°C, at which the PP matrix began to crystallize, the value of ΔH_m for PA6 particles was nearly the same as the value of samples annealed at 50°C. At a given annealing temperature, the ΔH_m of PA6 particles decreased with decreasing the total amount of heterogeneities in the system. Annealing time seemed to have very little effect on ΔH_m of PA6 particles within the specified time scale, whether the annealing temperature was 120 or 135 or 150°C.

Similar results are also be found in Table 4; the melting temperature of PA6 decreased with decreasing the total amount of heterogeneities in the system, and for a given blend sample, the melting temperature of PA6 decreased with increasing the annealing temperature, independent of the annealing time duration. As for the reduction of the melting temperature, some researchers[22] suggested that it was due to the formation of γ-form crystals of PA6 because the melting point of γ-form (215°C) crystals was lower than that of

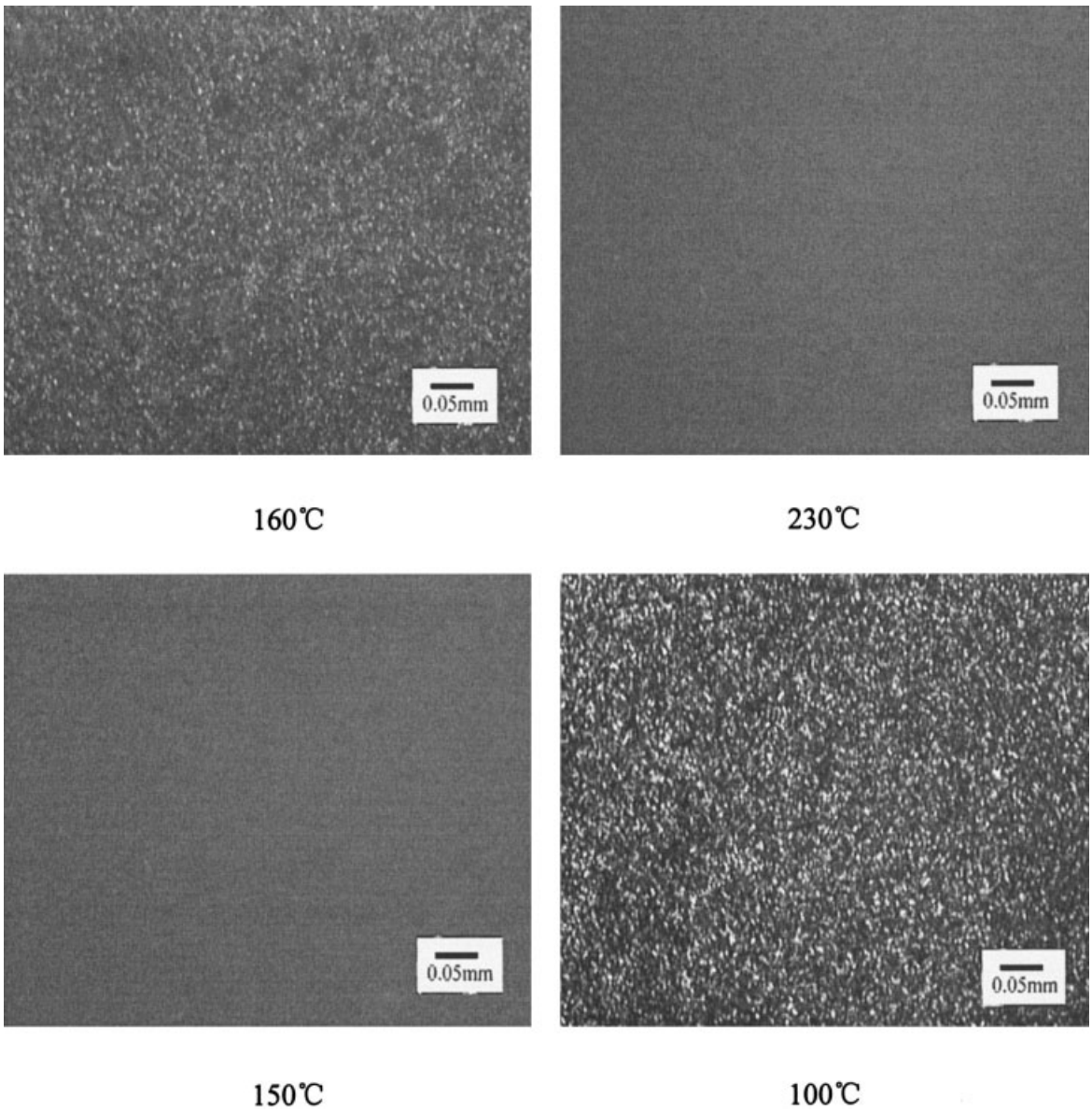

Figure 3 (*Continued from the previous page*)

α-form (221°C)[22,23] crystals. This explanation seems unlikely; according to our tests, the lowest melting temperature of PA6 particles was 194°C, which was much lower than that of the γ-form crystal. On the other hand, it is well known that the melting temperature of crystallizing polymers also depends largely upon the crystals lamella thickness as well as its architecture structure.[24] The decrease of the melting temperature could be tentatively attributed to the reduction of perfection and thickness of PA6 crystals.[20] This indicats that crystals activated by less efficient nuclei and formed under higher supercooling crystallization temperatures should have more defects in the crystal structures than those formed under the usual crystallization temperature.

Polarized light microscope (PLM) micrographs of some PP/PP-*g*-MAH/PA6 blends listed in Figure 3 might also favor the above-mentioned point of view. They are the samples A, B, C, and D listed in Table I. The four samples were heated to 160°C and held for 5 min before reaching 230°C. After holding at 230°C for 5 min, these samples were cooled to 150°C at 10°C/min and held for 5 min before being further cooled to 100°C. Photographs were taken at 160, 230, 150, and 100°C, respectively. From Table I, we could see that samples A and B could not be extracted and samples C and D were extractable. Comparing the figure from samples A and B, and samples C and D, differences are easily found. Although the existence of PP-*g*-MAH-*g*-PA6 in sample B made the dispersion particle much smaller, we could still find many PA6 crystals at 150°C. But in the photos of samples C and D, we see hardly any evidence of crystallization. In Table II, it is seen that sample B had almost the same dispersed

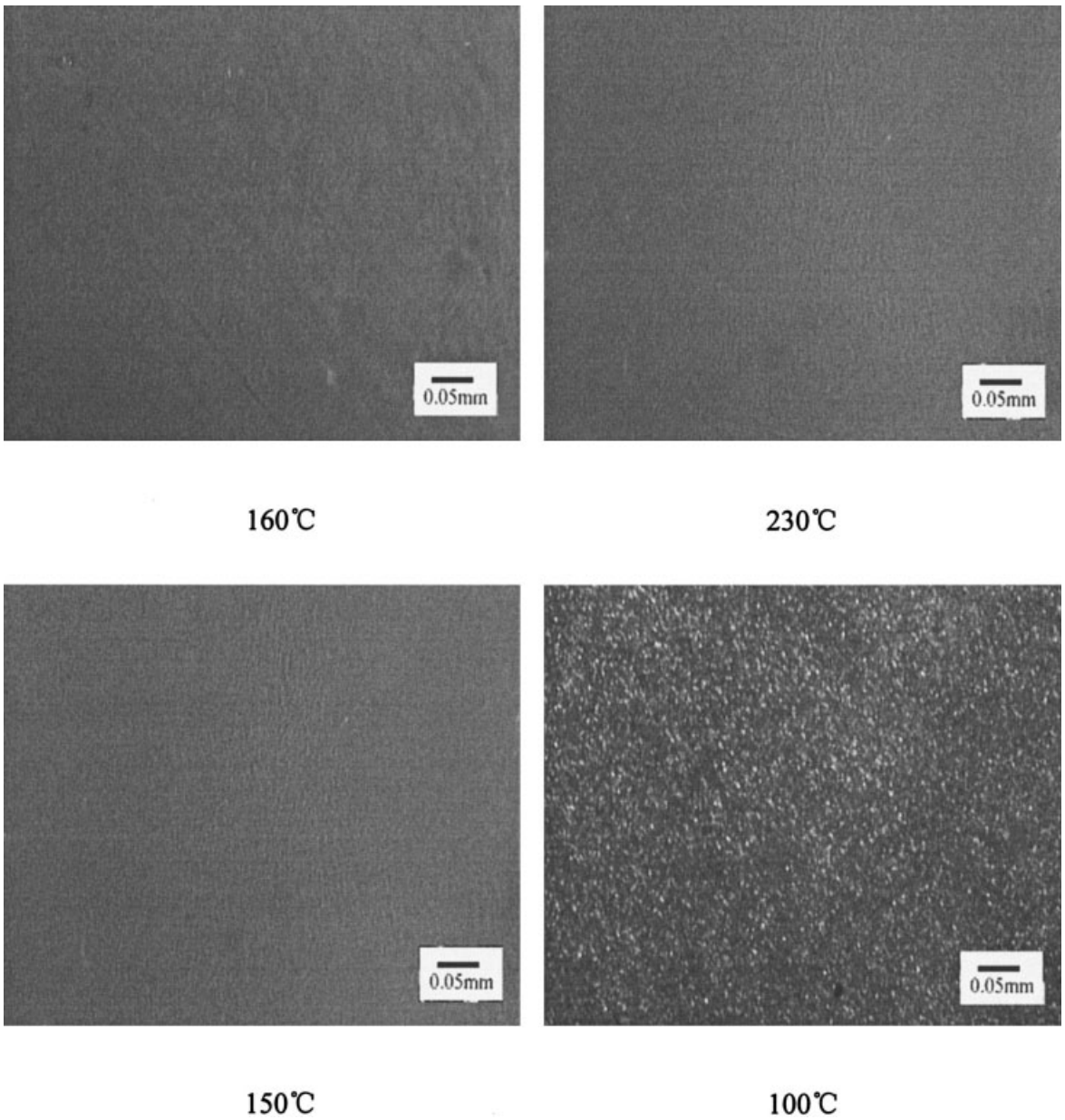

Figure 3 (*Continued from the previous page*)

particle size level as samples C and D. A lack of active heterogeneities might be the major reason for this experimental result.

Referring to the experimental results obtained in Figure 1, for the blends of 0/70/30, the crystallization peak of PP was lower than that in the blend of 80/0/20 [see Fig. 1(a)]. This can be tentatively ascribed to the following two possible factors: (1) migration of heterogeneities in the blending system: according to a previous report, nuclei migration would take place during mixing of the blend in the molten state. The driving force for it is the difference of the interfacial energies of impurities with respect to each molten component in the blends.[25] If the interfacial free energy of such a potential nuclei with respect to component A was higher than that with respect to component B, then the nuclei would pass across the interface to enter into the phase of component B during melt mixing. Because most of the impurities existing in our system should have polar surfaces, the interfacial free energy between the impurity nuclei and PA6 phase might be lower than that between the nuclei and the PP phase. So, during melt mixing, the nuclei would tend to migrate from the PP phase to the PA6 phase. But, in uncompatibilized blends, the interface between PA6 and PP was very sharp and clear. The interface area was also relatively small because of the relatively larger dispersed droplets size. The interfacial tension and interfacial energy were all relatively higher, which would prohibit the migration of impurity nuclei. Conversely, in compatibilized blends, owing to the vague interface and lower interfacial tension, in-

terfacial energy, and larger interface area, the migration of impurity nuclei was easier. In that case, more and more active heterogeneities would migrate from the molten PP phase to the PA6 phase during melt mixing. The remained heterogeneities in the PP matrix of the compatibilized system would be lower than that in the uncompatibilized blends, so the crystallization temperature of PP would decrease accordingly. (2) PA6 crystals in the compatibilized blends should have a weaker nucleation effect on the PP's crystallization. As in compatibilized blends, the interface between the PA6 and the PP phase became more vague, so the nucleation effect of the interface on PP was weaker than for the uncompatibilized system. This might be another reason for lower crystallization temperature in compatibilized blends.

The following self-seeding experiments also illustrate some positive results to this point. Generally speaking, the fractionated crystallization behavior of the dispersed PA6 phase was due to the lack of active heterogeneity nuclei in the PA6 particles. If nucleating agents were added to the blending system, the fractionated crystallization would become weaker or even disappear.[12] The procedure to induce self-crystallization consisted of the following steps: (a) erasure of previous thermal history by heating the sample at 200°C for 5 min; (b) creation of a "standard" thermal history by cooling at 10°C/min to 0°C; (c) heating up to a temperature T_s; (d) thermal conditioning at T_s for 5 min; (e) DSC cooling scan from T_s down to 0°C at 10°C/min, where the effects of the thermal treatment will be reflected on the crystallization of the blends. To study the effect of different heterogeneities, the following two blends were prepared for this self-seeding test. 60/10/30 (d_v = 0.42 μm, D = 1.34) and 80/10/10 (d_v = 0.2 μm, D=1.02). It was found that the dispersed particles of the blend, which had 30%, PA6 content,

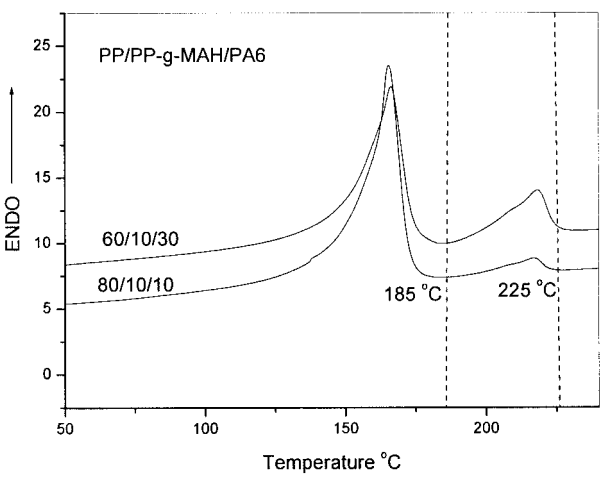

Figure 4 DSC heating scans (10°C/min) of blends 80/10/10 and 60/10/30 (erasing the thermal history by heating to 250°C and holding for 5min and then cooling to room temperature at 10°C/min before testing).

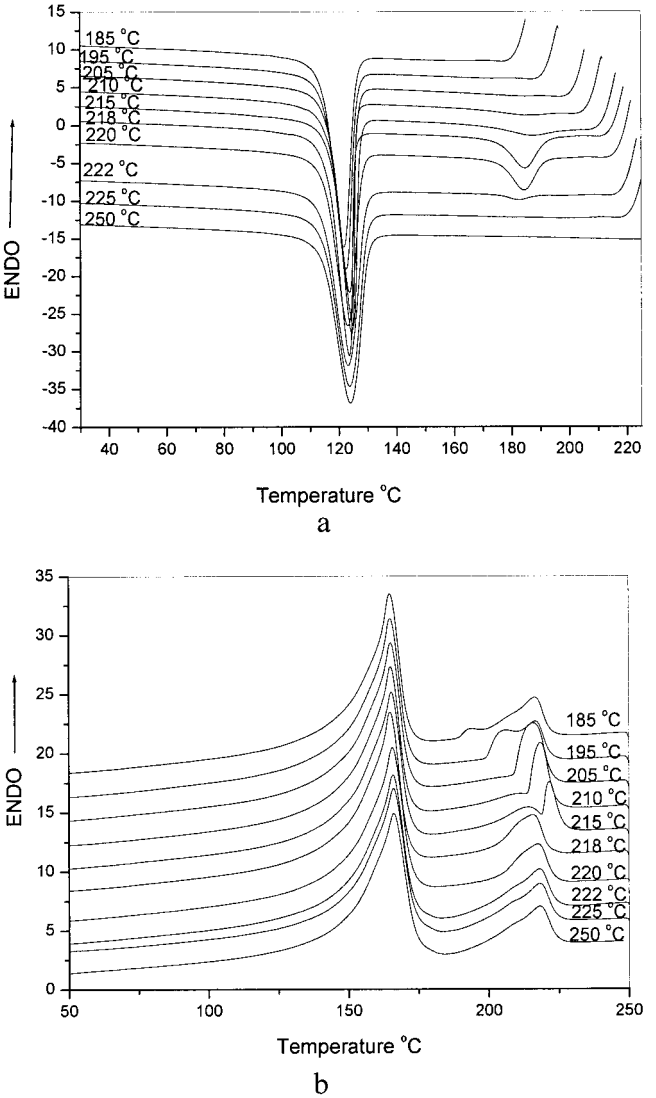

Figure 5 (a) Cooling DSC scans (10°C/min) from the indicated T_s temperature for 60/10/30 blend; (b) subsequent heating DSC scan (10°C/min) after self-nucleation at the indicated temperature.

were almost double in size of those in blend 80/10/10. As the number of original heterogeneities in PA6 (about 2×10^{12} nuclei/cm^3),[2] were much larger than those in PP (about 9×10^6 nuclei/cm^3),[26] so the migration of nuclei from the PP phase to the PA6 phase would have very little effect on the total nuclei in the PA6 phase in the above two blends. It can be assumed that more particles in blends 80/10/10 would contain less active heterogeneous nuclei. According to the heating thermogram in Figure 4, nine self-nucleation temperatures (T_s) between 185 and 225°C were selected in the experiment: they were 185, 195, 200, 205, 215, 218, 220, 222, and 225°C, respectively. All the samples were first heated to 250°C, held for 5 min, and then cooled to room temperature before testing so that the thermohistory would be the same. The cooling thermograms are shown in Figures 5 and 6. According

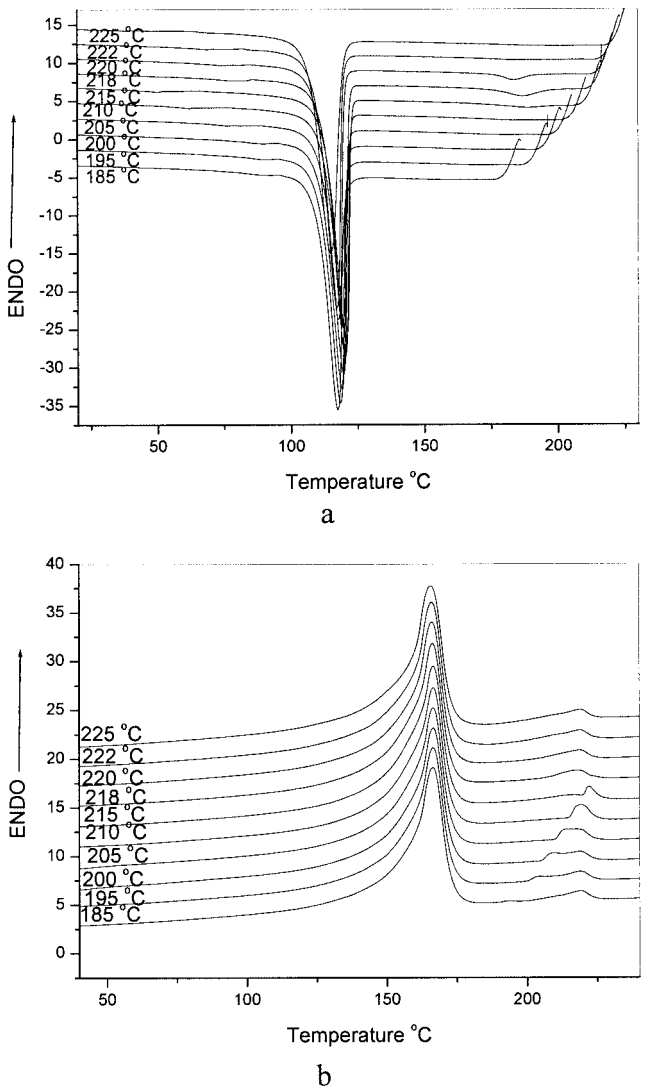

Figure 6 (a) Cooling DSC scans (10°C/min) from the indicated T_s temperature for 80/10/10 blend; (b) subsequent heating DSC scan (10°C/min) after self-nucleation at the indicated temperature.

to ref. 27, three domains describe the self-nucleation temperature T_s. If T_s is too high, the sample is said to be in "domain I" or the complete melting domain. When T_s is high enough to almost completely melt the sample but low enough to leave small crystal fragments that can act as self-nuclei during the subsequent cooling from T_s, the sample is said to be in "domain II," or the self-nucleation domain. When T_s is too low, only part of the crystal population will be melted, and therefore, the unmelted crystals will be annealed during the 5 min at T_s while the rest of the polymer will be self-nucleated during the subsequent cooling from T_s, then the sample is said to be in "domain III," or the self-nucleation and annealing domain.

According to the theory of refs. 27 and 28, it could be easily found that, in blends 60/10/30, domain II began at 222°C, and domain III began at 215°C; but in blends PP/PP-*g*-MAH/PA6 = 80/10/10, domain II started at 220°C and domain III was also at 215°C. This indicates that the crystals formed with less active nuclei at higher supercooling would have lower melting temperatures than those formed at lower supercooling temperatures. This result is further supported by the following WAXD experiment.

Figure 7 lists the experimental results obtained by a WAXD test. The spectra were obtained at 180°C. All diffraction peaks could be attributed to the contribution of PA6, because PP was in the melt state at this temperature. The average volume particle diameter in blends 40/40/20 was $d_v = 0.28$ μm, $D = 1.04$, which is very close to that of 0/80/20 listed in Table II; these two samples were unextracted, so the distribution of heterogeneities in the two blends should be at the same level. It can also be found that the relative diffraction peak intensities in the two blends were almost the same. But for the extracted sample, in which most of the heterogeneities nuclei had been removed, the intensity of PA6 diffraction peaks decreased sharply and became almost invisible. From the DSC heating curve of sample D listed in Figure 8, we see that the PA6 crystals in the blends did not melt at testing temperature. This indicates that the crystals in sample D, which were formed with less active nuclei, might have less perfect structures than those in the 40/40/20 and 0/80/20 blends.

Furthermore, we noticed a very small exothermic peak below 100°C in the cooling curve obtained from the self-nucleation test: a magnification of the corresponding area is shown in Figure 9. All these small crystallization peaks were thought to be fractionated crystallization exotherm peaks of PP. According to our previous work, the existence of the PA6 phase in the PP/PP-*g*-MAH/PA6 blending system might induce phase separation of PP and PP-*g*-MAH and form the emulsion-in–emulsion structure in the system.[29] The

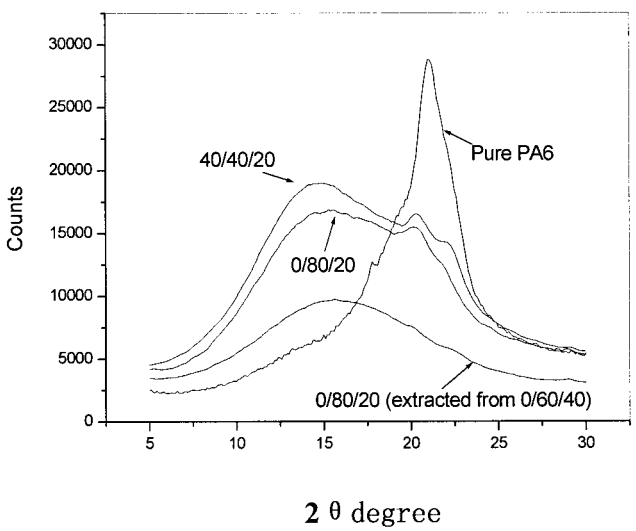

Figure 7 WAXD patterns of pure PA6 and PP/PP-*g*-MAH/PA6 blends (testing temperature 180°C).

small crystallization peak showen in Figure 9 should come from the fractionated crystallization of PP-*g*-MAH droplets encapsulated by the PA6 phase and separated from the matrix by the PA6 droplets (see Fig. 8 in ref. 32). Further detailed investigation of this enclosed droplet crystallization is under way in our laboratory.

It is well known that PA6 grafted onto PP backbones in the PP-*g*-MAH-*g*-PA6 copolymer has different crystallization behavior from the dissociated phase.[30,31] We also have an increasing trend of the PP-*g*-MAH-*g*-PA6 copolymer content from sample B to F, but as its absolute content was too low, so we did not detect any signals for crystallization of grafted PA6 chains or its effects on the dissociated PA6's crystallization behavior.

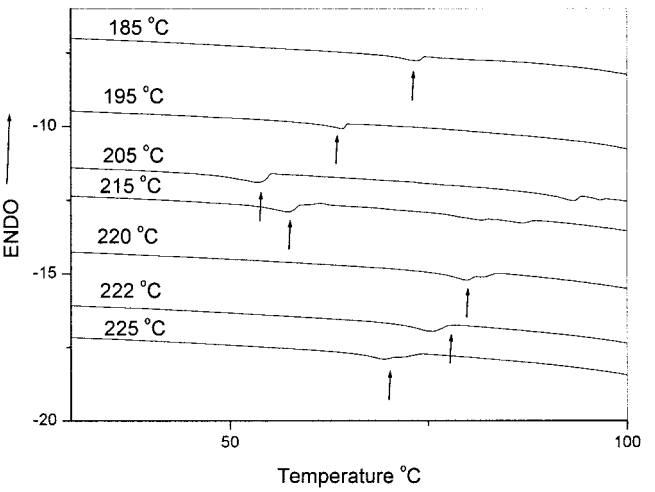

Figure 9 Magnified curve of Figure 5 (a) in 30–100°C area.

CONCLUSION

1. Fractionated crystallization behavior of PA6 was observed in a PP/PP-***g*-MAH/PA6 blend system when PP or PP-***g***-MAH was the matrix and PA6 was in domains.
2. The lack of normal active heterogeneities in the dispersed droplets was the key factor in the fractionated crystallization of PA6.
3. The crystals formed with less efficient nuclei might contain more defects in the crystal structures than those crystallized with usual active nuclei. The lower the crystallization temperature, the less perfection of the crystals and the lower crystallinity would be.
4. The crystallization of grafted PA6 chains in the PP-*g*-MAH-*g*-PA6 copolymer or its effects on the dissociated PA6's crystallization behavior was not detected.
5. The fractionated crystallization of PP droplets encapsulated by PA6 domains was also observed.

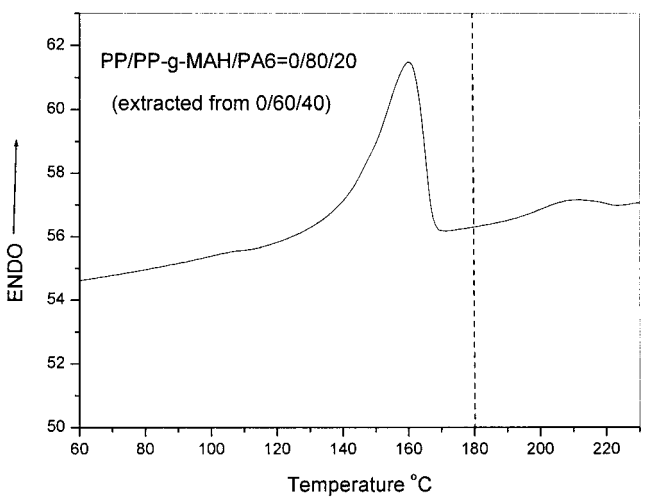

Figure 8 DSC heating scans (10°C/min) of blends 0/80/20 (extracted from 0/60/40) (erasing the thermal history by heating to 250°C and holding for 5min and then cooling to room temperature at 10°C/min before testing).

Much appreciation is given to Professor Stephen Z. D. Cheng, The University of Akron, OH; Professor Hu Guohua, Laboratoire des Sciences du Génie Chimique, Ecole Européenne d'Ingénieurs en Génie des Matériaux, France, and Professor G. C. Alfonso, Department of Chemistry and Industry Chemistry, University of Genova, Italy, who have given very useful suggestions and discussion to this article.

References

1. Frensch, H.; Harnischfeger, P.; Jungnickel, B. J. In Multiphase Polymer: Blends and Ionomers; Utracki, L. A.; Weiss, R. A., Eds.; ACS Symp. Ser. 395; American Chemical Society: Washington, DC, 1989.
2. Frensch, H.; Jungnickel, B.-J. Colloid Polym Sci 1989, 264, 16.
3. Frensch, H.; Jungnickel, B.-J. Plast Rubber Comp Proc Appl 1991, 5, 16.
4. Klemmer, N.; Jungnickel, B.-J. Colloid Polym Sci 1984, 262, 381.
5. Tsebrenko, M. V. Int J Polym Mater 1963, 10, 83.
6. Baitoul, M.; Saint-Guirons, H.; Xans, P.; Monge, P. Eur Polym J 1981, 17, 1281.
7. Ikkala, O. T.; Holsti-Miettinen, R. M.; Seppala, J. J Appl Polym Sci 1993, 49, 1165.
8. Arnal, M. L.; Matos, M. E.; Morales, R. A.; Santana, O. O.; Muller, A. J. Macromol Chem Phys 1998, 199, 2275.
9. Jafari, S. H.; Gupta, A. K. J Appl Polym Sci 1999, 71, 1153.
10. Manaure, A. C.; Morales, R. A.; Sanchez, J. J.; Muller, A. J. J Appl Polym Sci 1997, 66, 2481.
11. Jafari, S. H.; Gupta, A. K.; Rana, S. K. J Appl Polym Sci 2000, 75, 1769.
12. Morales, R. A.; Arnal, M. L.; Müller, A. J. Polym Bull 1995, 35, 379.
13. Moon, H. S.; Ryoo, B. K.; Park, J. K. J Polym Sci Part B Polym Phys 1994, 32, 1427.
14. Everaert, V.; Groenincks, G.; Aerts, L. Polymer 2000, 41, 1409.
15. Manaure, A. C.; Morales, R. A.; Sanchez, J. J.; Muller, A. J. J Appl Polym Sci 1997, 66, 2481.
16. Santana, O. O.; Müller, A. J. Polym Bull 1994, 32, 471.
17. Morales, R. A.; Arnal, M. L.; Muller, A. J. Polym Bull 1995, 35, 379.

18. Manaure, A. C.; Muller, A. J. Macromol Chem Phys 2000, 201, 958.
19. Sánchez, A.; Rosales, C.; Laredo, E.; Muller, A. J.; Pracella, M. Macromol Chem Phys 2001, 202, 2461.
20. Schultz, J. M. Polymer Materials Science; Prentice-Hall, Inc.: Englewood Cliffs, NJ, 1974.
21. Chandrasekar, S. Res Mod Phys 1943, 15.
22. Hirami, I. M. J Macromol Sci Phys 1984–1985, B23, 397.
23. Reimschuessel, H. K. J Polym Sci Macromol Rev 1977, 12, 65.
24. Wunderich, B. Macromolecular Physics; Academic Press Inc.: New York, 1980, Vol. 3, Chap IX.
25. Bartczak, Z.; Galeski, A.; Krasnikova, N. P. Polymer 1987, 26, 1627.
26. Fillon, B.; Wittman, J. C.; Lotz, B.; Therry, A. J Polym Sci Part B Polym Phys 1993, 31, 1383.
27. Arnal, M. L.; Muller, A. J. Macromol Chem Phys 1999, 200, 2559.
28. Arnal, M. L.; Muller, A. J.; Maiti, P.; Hikosaka, M. Macromol Chem Phys 2000, 201, 2493.
29. Shi, D.; Ke, Z.; Yang, J.; Gao, Y.; Wu, J.; Yin, J. Macromolecules 2002, 35, 8005.
30. Loo, Y. L.; Register, R. A.; Ryan, A. J. Macromolecules 2002, 35, 2365.
31. Albuerne, J.; Ma' rquez, L.; Muuller, A. J. Macromolecules 2003, 36, 1633.